Experimental measurement of thermal, electrical, and chemical properties of materials for applications in data storage and chemical sensing

Ranjan Grover

College of Optical Sciences
University of Arizona

Post-doctoral candidate

Tucson: Home of the truly macroscopic wavefunctions

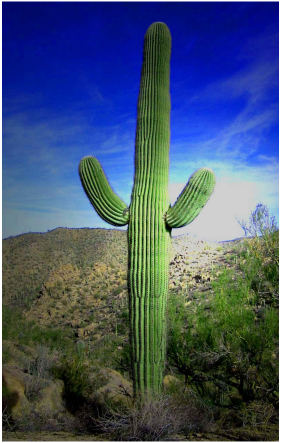

Figure: A Saguaro cactus. Its momentum and position are quite easy to measure simultaneously.

Talk outline

Motivation for nanoscale thermal and electrical measurements

- Applications in ultrahigh density ($> 1\mathrm{Tb}/\mathrm{in}^2$) magnetic data storage.
- Thermal management in silicon processors which will soon have interconnects with sub 50 nm line widths.
- Interesting science in thermal heat transport at the nanoscale particularly in electron-phonon interactions, photon-vibrational interactions, etc.

How much information

Some figures

- New Information Stored in 2002 = 5 Exabytes = 5×10^{18} bytes (growing 30% per year).
- The Stanford linear accelerator is the world's largest single database at 500 TB.
- Magnetic (92%), Film, Paper, Optical.

Citation

Source:
http://sims.berkeley.edu/research/projects/how-much-info-2003.

The superparamagnetic limit

As bits shrink, amount of magnetic energy stored reduces, and the bits can be flipped due to ambient thermal energy. This is the superparamagnetic limit.

Trends in the magnetic storage industry

- Longitudinal recording: Bits in the plane of the film. Maxed out at $\sim$100 Gbit/in^2.
- Perpendicular recording: Bits perpendicular to the plane of the film. More magnetic energy stored per bit. Expected to max out at 400 Gbit/in^2.

Heat assisted magnetic recording

- Variant of perpendicular recording.
- Uses magnetic materials with high coercivity.
- Requires localized heating for recording.
- Expected to reach 1 $Tbit/in^2$ and beyond. The bit pitch for 1 $Tbit/in^2$ is 25 nm.

Heat assisted magnetic recording (HAMR)

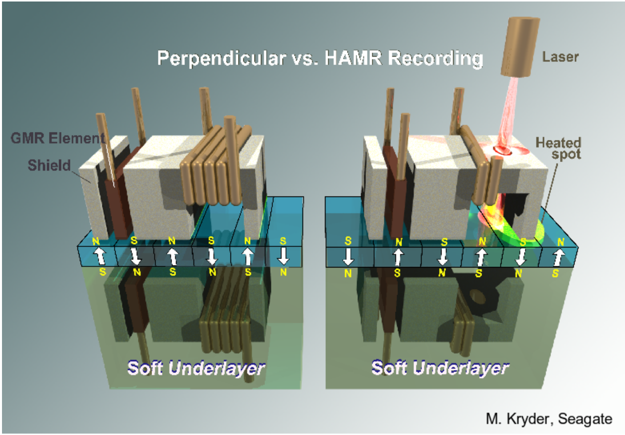

Figure: A comparison of system topologies of perpendicular magnetic recording and heat assisted magnetic recording. *Acknowledgement: Mark Kryder, Seagate.*

Roadmap

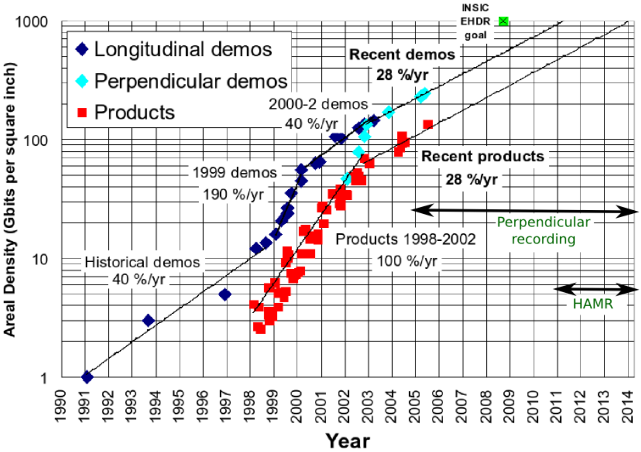

Figure: Perpendicular recording should work till 400 Gbit/in^2. HAMR is at least 5 years away and still has many unsolved issues. *Acknowledgement: Barry Schechtman, Insic.*

1 Tbit/in^2 is a LOT of information!

Figure: With 1 Tbit/in^2 you can store the picture of every man, woman, and child on earth on a disc the size of a compact disk.

Figure: 750 bytes, 30x30 pixel, 8 bit grayscale, jpeg compression. *Acknowledgement: Tim Rausch, Seagate*.

Part I: Nanoscale temperature measurement

Delivering heat locally

- An AFM cantilever may be used to heat locally by raising its temperature using a laser beam.
- Demonstrated by Wickramasinghe and co-workers at IBM.
- We sought out to measure the temperature of the AFM cantilever using Raman methods.

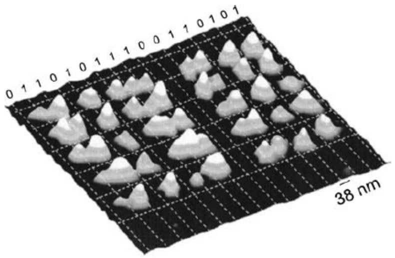

Figure: HAMR using a heated AFM cantilever.

Raman measurements

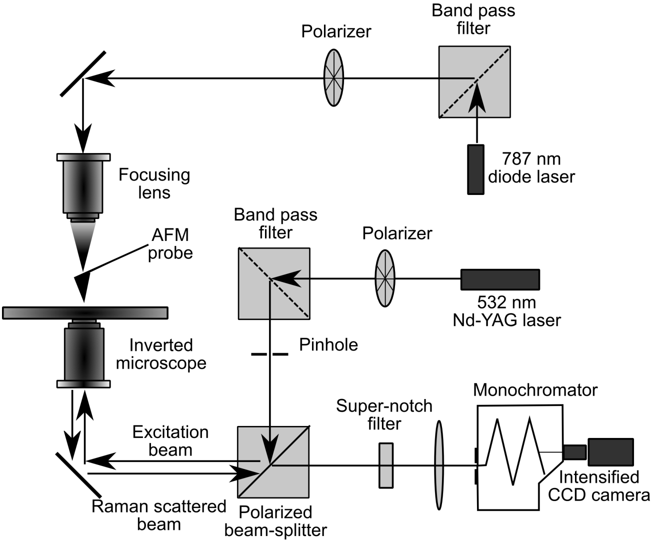

Figure: Raman setup for measuring temperature of a heated AFM cantilever.

Governing equations

$$n = \frac{n_S}{n_{aS}} \propto \exp\left(\frac{h\Delta\nu}{kT}\right)$$

where h and k are the Planck and Boltzmann constants and n_{S} and n_{aS} are the Stokes and anti-Stokes intensities respectively.

$$T = \frac{h}{k}\frac{\Delta E}{\log\left(\sigma \frac{n_{\mathrm{S}}}{n_{\mathrm{aS}}} \frac{(E_0 + \Delta E)^3}{(E_0 - \Delta E)^3}\right)}$$

E_0 and ΔE are the laser energy and the energy of the Raman shift, and σ is a correction factor that accounts for the difference in the temperature dependence of the Raman cross-sections and optical absorptions at the anti-Stokes and Stokes wavelengths, equalling approximately 0.87.

Experimental Results

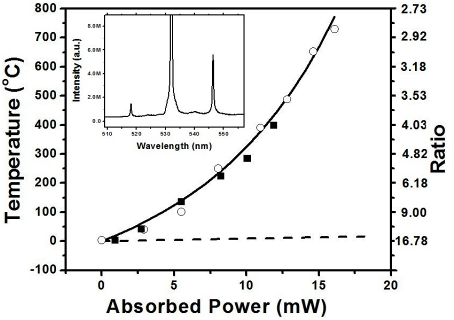

Figure: The silicon cantilever tip anti-Stokes/Stokes ratio and derived temperature measured by the Raman scattering system for two configurations: (a) pumping and probing the tip using a 532 nm laser (■) and (b) pumping the back of the cantilever with a 787 nm laser and probing the tip with a 532 nm laser (◯). The solid line is a fit to the experimental data while the dotted line is the temperature rise for a bulk silicon sample under the same heating conditions. The inset shows a typical Raman spectrum obtained with our experimental setup.

Experimental Results

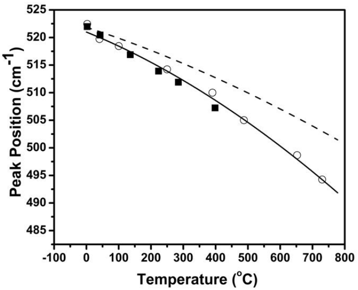

Figure: The peak position of the Stokes (and anti-Stokes) energy as a function of temperature, T, for a bulk silicon sample (dashed line) and as measured on the silicon tip, corresponding to the measurements of the previous figure.

Thermal interface in HAMR media

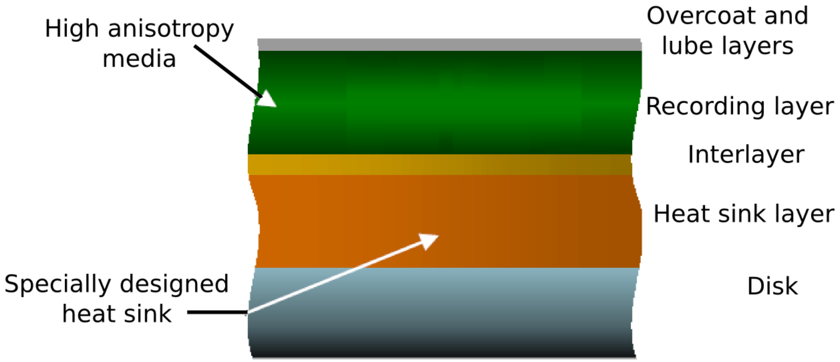

Figure: Special high temperature lubes have been developed to combat high temperatures. The heat sink layer is introduced to take away the heat more efficiently. Interface effects are seen between the overcoat/lube, mag layer and heat sink layer since spot size is 25 nm. *Acknowledgement: R. Rottmayer, Seagate.*

Thermal microscopy using bimetallic cantilevers

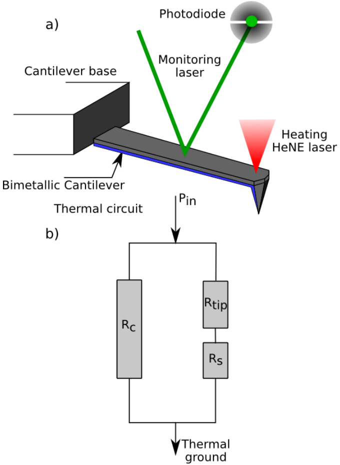

Figure: a) Bimetallic cantilever and coupled heating laser for thermal microscopy b) Corresponding thermal circuit, R_c, R_t, and R_s, are the cantilever, tip, and sample thermal resistances.

κ-AFM elements

- Si-Pt bimetallic cantilever
- An extra heating (HeNe)laser
- Exploits the differences in the bending profile of cantilever bent due to bimetallic deformation, and a cantilever which is bent purely by a force setpoint

AFM: Basic concepts

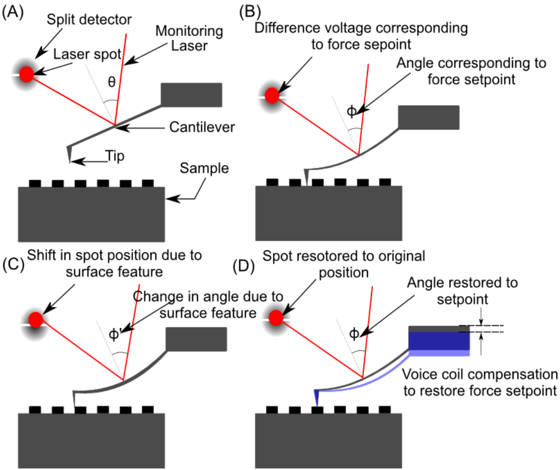

Figure: Basic illustration of a AFM using optical read-out

How it works

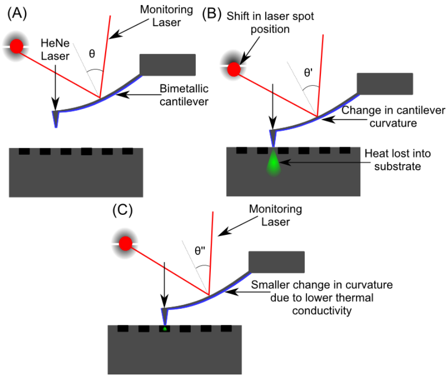

Figure: Principles of operation of UoA Scanning thermal microscope

Note

Two scans are done, one with a cold followed by a hot cantilever

Imaging a grating with Si and SiO_2

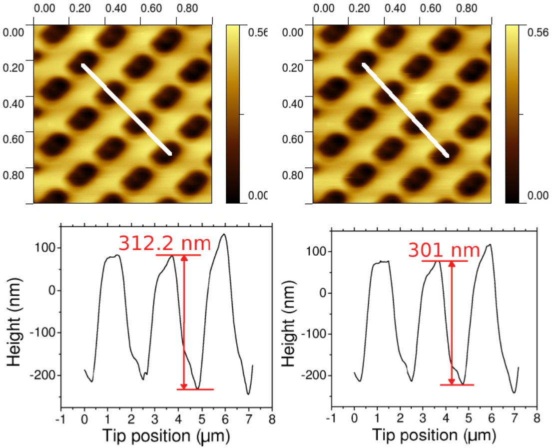

Figure: Si - dark features and SiO_2 light features

Checking for convective cooling

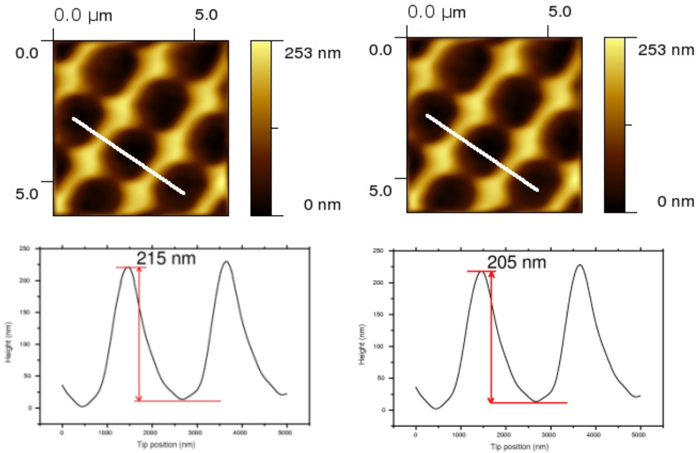

Figure: Etched version of previous sample, now with a much lower step height

Imaging a grating with only SiO_2 features

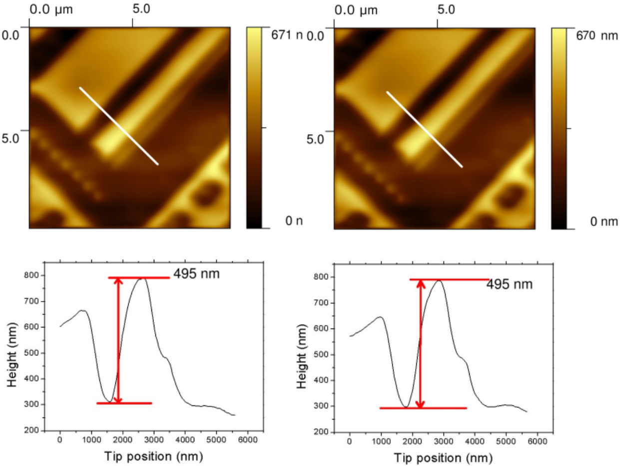

Figure: SiO_2 on both light and dark regions

Optimizing the thermal circuit using nitride cantilevers

Figure: V-shaped silicon nitride cantilever with a silicon tip at the end

Description

- V-shaped cantilever, 200 μm in length, 35 μm width of each arm, 1 μm thick, made of Si_3N_4
- Tip height is 10 μm, made of Si
- Si_3N_4 has a thermal conductivity which is 5X lower than Si. Thus the topographic distortion seen from this cantilever-tip system will be 5X larger

Summary and Conclusions, Part I

- A new instrument is developed and shows contrast between features of different thermal conductivity.
- The system can be analyzed with a simple analytical model.
- The sample is heated locally, the exact local power absorbed is known and thus, local thermal conductivity values can be extracted.
- The spatial resolution for the thermal resolution is limited to 100 nm because of interface effects.

Part II: Electrical probe storage on phase-change media

The IBM Millipede

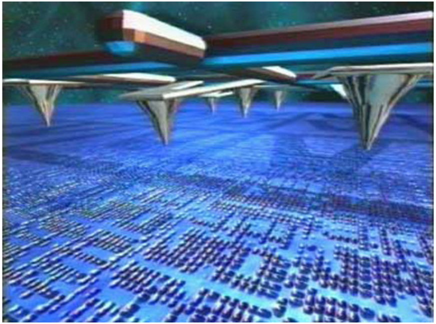

Figure: The IBM Millipede. 1024 cantilevers working in parallel. Data is stored by creating pits on a polymer media using a heated AFM tip.

Storing data bits using conductance switching

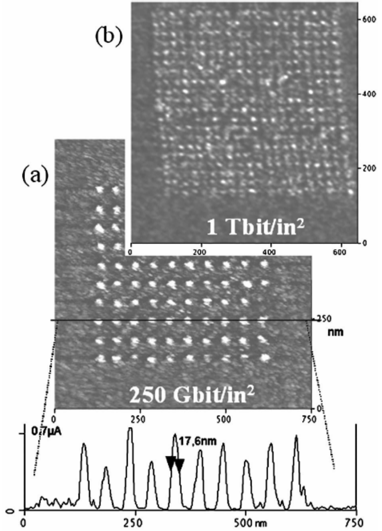

Figure: Storing data bits as crystalline and amorphous regions. Gidon *et. al*

System overview

- Data storage is done by changing the phase of phase change media.
- The crystalline phase, and the amorphous phase vary in resistivity by 3 orders of magnitude.
- System uses a large array of conducting probes to increase throughput.

Media

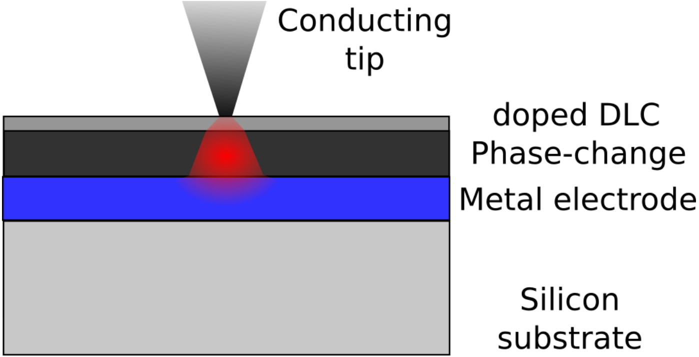

Figure: Proposed media thin-film stack.

Challenges

- Establishing ohmic contact reproducibly with an AFM tip.
- Tip loses conductivity due to frictional and current-induced damage.
- Modeling the system is a challenge because of point contact effects and ballistic electron transport through nanoconstrictions.

The capping layer

- Phase change media oxidizes on exposure to the ambient.
- Amorphous carbon media has been proposed to act as overcoat media.
- There is a need to control overcoat conductivity to maximize contrast.
- Overcoat needs to be thin (sub 10 nm) and conducting.

IV curves on diamond like carbon (DLC) sample

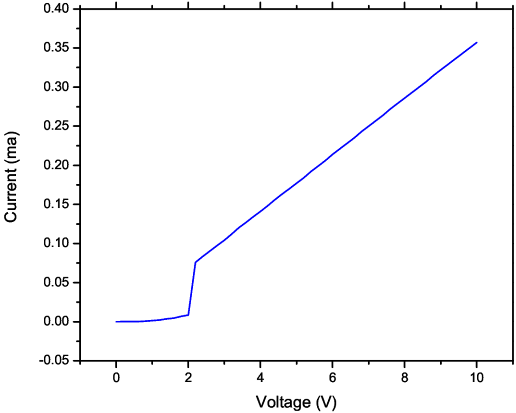

Figure: IV curves on Nanochip media sample: Metal electrode + DLC

Establishing contact with pulses

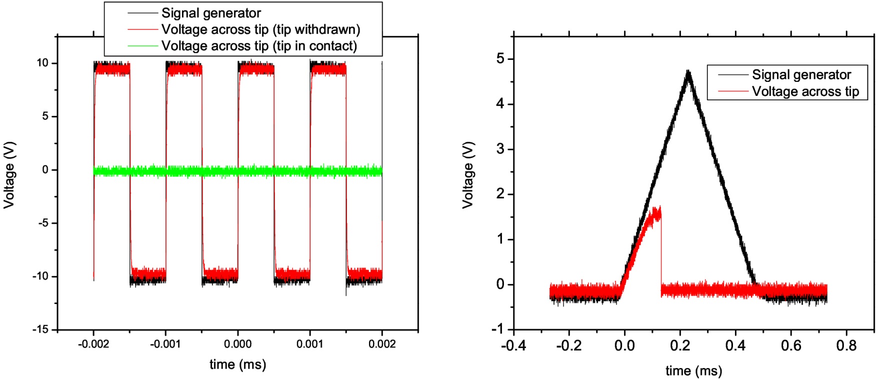

Figure: Triangular and square pulses on Nanochip media sample: Metal electrode + DLC

Post IV curve imaging

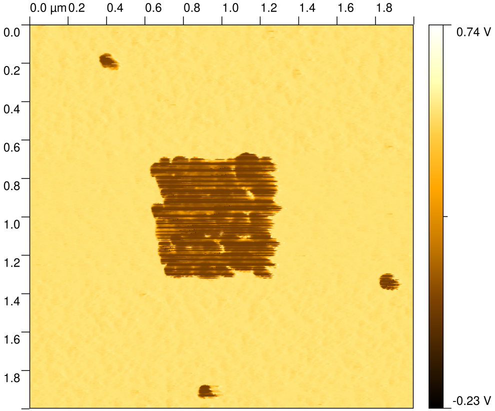

Figure: A 500 nm square is scanned with a high field to break down the local dielectric impurity and then a larger area around it is scanned to see the effect on the topographical and electrical maps. The square is where ohmic contact is established and outside it, we have FN tunneling.

Summary and Conclusion, Part II

- Surface contaminants inhibit ohmic contact at a low applied field.
- Ohmic contact can be established at high fields which breaks down the dielectric contamination.
- Tip damage over a period of time is a very real problem. Most of the damage is frictional for lower current densities.
- Due to ballistic electronic transport through nanoconstrictions, role of each layer in the thin film stack is hard to determine. Thus modeling becomes difficult.

Part III: Measuring workfunction using Kelvin probe force microscopy

The need for effective chemical sensing

Applications

- Defense applications.
- Quality control in labs and manufacturing environment.

Requirements of future chemical sensors

- Need to better sub-ppb sensitivity.
- Goal to have chemical sensors on a chip.

Chemical sensing using ChemFETs

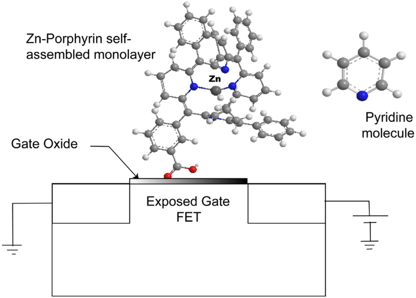

Figure: Open gate MOSFET with a chemically sensitive monolayer. On reaction, the workfunction shifts which leads to a change in the the gate workfunction, and the output IV characteristics of the transistor.

Characterizing the monolayer

Measurement of the spatial and temporal response of the monolayer on exposure to gas is an important area of research to make this device viable.

Contact potential difference

$$V_{\text{CPD}} = \phi_1 - \phi_2$$

where ϕ_i is the workfunction of the material i

Kelvin probe

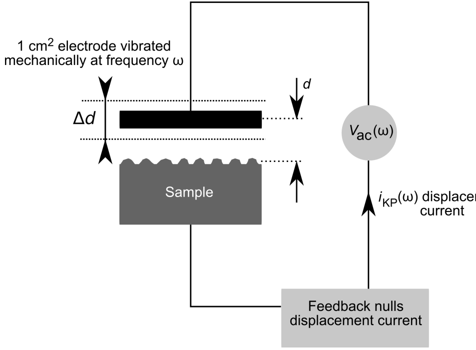

Figure: A Kelvin probe can determine workfunction change.

$$C_{\mathrm{KP}} = \epsilon_0 \frac{A}{d}\left(1 - \frac{\Delta d}{d}\sin\omega t\right)$$

V_{ex} is the dc voltage from the feedback system.

$$i_{\mathrm{KP}}(t) \propto \epsilon \frac{A}{d^2}\omega(V_{\mathrm{CPD}} - V_{\mathrm{ex}})\Delta d \sin\omega t$$

Kelvin probe force microscopy

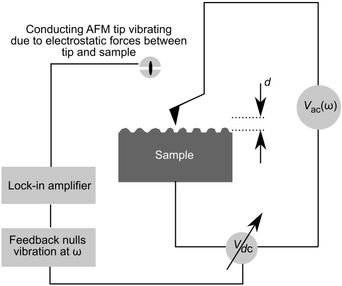

Figure: A Kelvin probe force microscope can determine local workfunction change with near atomic resolution.

V_{ex} is the dc voltage from the feedback system

$$i_{\mathrm{KPFM}}(t) \propto \epsilon \frac{r}{d} \frac{2\pi}{\kappa} (V_{\mathrm{CPD}} - V_{\mathrm{ex}}) V_{\mathrm{ts}} \sin \omega t$$

Experimental Results

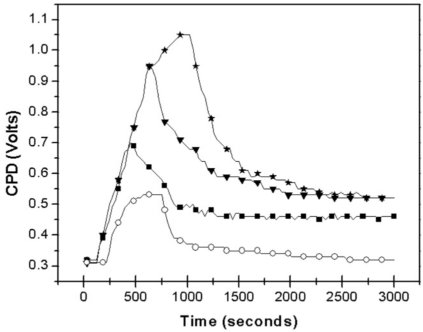

Figure: Temporal evolution of CPD versus time for FBP and ZnP on exposure to pyridine gas. ★ZnP exposed to pyridine for ∼16 minutes. ▼ZnP exposed to pyridine for ∼11 minutes.■ZnP exposed to pyridine for ∼9 minutes. ◯FBP exposed to pyridine for ∼12 minutes. It may be noted here that the FBP data is offset by 0.62 V for clarity.

Results continued

Table: Experimental results performed with a Kelvin Probe Force Microscope (KPFM) and a Kelvin Probe (KP) on self-assembled monolayers of free-base porphyrin (FBP) and Zn-porphyrin(ZnP) before and after exposure to a pyridine gas. Note that the CPD measurements for the exposed samples are done one hour after exposure to pyridine and that the CPD values have reached a steady state. The results summarized here are consistent with those seen in Fig. 27

Sample	CPD(V) KPFM	CPD(V) KP6500
FBP	-0.303 $\pm$ 2.5%	-0.31 $\pm$ 2.1%
FBP+Pyridine	-0.31 $\pm$ 3.1%	-0.30 $\pm$ 4.1%
CPD Shift	-0.097	0.1
ZnP	0.348 $\pm$ 4.3%	0.31 $\pm$ 2.35%
ZnP+Pyridine	0.557 $\pm$ 3.2%	0.52 $\pm$ 3.2 %
CPD shift	0.209	0.21

Summary and Conclusions, Part III

- A Kelvin probe force microscope instrument was developed.
- The utility of the system in temporal and spatial evolution of CPD is demonstrated.
- The utility of this instrument is in evaluating the response of specific chemically sensitive monolayers on exposure to gas in real-time.

The evolution of the AFM

Figure: Optical data storage is one commercial aspect of optical microscopy.

The AFM has rapily evolved from a lab analysis instrument to the enabling technology for next generation instrumentation. Its uses are limited only by our imagination.

Acknowledgements

- Prof. Dror Sarid: Academic advisor.
- Dr. Brendan McCarthy: colleague, Thermal microscopy project.
- Dr. Pramod K. Khulbe: colleague, Probe storage project.
- NSF, Seagate, and INSIC: for paying the bills.
- Various staff and faculty of the College of Optical Sciences who are too numerous to list.

Published work

- Ranjan Grover, Brendan McCarthy, Ibrahim Guven, and Dror Sarid, "Mapping thermal conductivity using bimetallic atomic force microscopy cantilevers," *Applied Physics Letters*, **88**, 233501 (2006).
- Dror Sarid, Brendan McCarthy, and Ranjan Grover, "Scanning Thermal Conductivity Microscope," *Review of Scientific Instruments*, **77**, 023703 (2006).
- Brendan McCarthy, Yanming Zhao, Ranjan Grover, and Dror Sarid, "Enhanced Raman scattering for temperature measurement of a laser-heated atomic force microscope tip," *Applied Physics Letters*, **86**, 111914 (2005).
- Two book chapters, Chapter 17 and 18 in Exploring Scanning Probe Microscopy with *Mathematica*, 2^{nd} Ed.
- R. Grover, B. McCarthy, Y. Zhao, G. E. Jabbour, D. Sarid, G. M. Laws, B. R. Takulapalli, T. J. Thornton, and D. Gust, "Kelvin probe force microscopy as a tool for characterizing chemical sensors," Applied Physics Letters, **85**, 3926 (2004)
- One book chapter, Chapter 19 in Exploring Scanning Probe Microscopy with *Mathematica*, 2^{nd} Ed.